Thermoelectric Power Factor of Ultra-Narrow Silicon Nanowires

N. Neophytou and H. Kosina
Institute for Microelectronics, Technical University of Vienna, TU Wien
Gußhausstraße 27-29/E360, A-1040 Wien, Austria.
e-mail: {neophytou|kosina}@iue.tuwien.ac.at

INTRODUCTION

The thermoelectric performance of materials is determined by the figure of merit ZT= $\sigma S^2/(\kappa_e+\kappa_l)$, where σ is the electrical conductivity, S is the Seebeck coefficient and κ_e and κ_l are the electronic and lattice contributions to the thermal conductivity, respectively. The interrelation of these quantities has traditionally kept ZT at low values, around unity. Nanomaterials have recently attracted significant attention because at the nanoscale the length scale degree of freedom offers possibilities of independent design of σ, S and κ_l such that high ZT values can be achieved. This was demonstrated to be the case not only for the rare-earth and/or toxic usual TE materials, but also for traditionally poor TE materials such as Si. Bulk Si has a very high κ_l=140W/mK which results in ZT~0.01 at 300K. Silicon nanowires (NWs), on the other hand, have demonstrated ZT~1 (Fig. 1) [1, 2], which makes Si a promising and abundant TE material candidate with well established industrial scale processes.

METHOD AND DISCUSSION

Although most of the ZT enhancement of Si NWs has resulted from the drastic reduction in κ_l down to 2W/mK, it is becoming evident that benefits from κ_l are reaching their limits, and further TE performance improvement will result from power factor (σS^2) improvements. In this work we present a comprehensive analysis of the thermoelectric power factor in Si NWs of different carrier type (n- and p-type), different diameters, and different transport and confinement orientations (Fig. 2). We employ the atomistic $sp^3d^5s^*$ tight-binding model and linearized Boltzmann transport theory [3]. We identify the design parameters that have the strongest influence on the power factor and identify bandstructure optimization directions. Our conclusions are of general relevance for the optimal design of the TE power factor of low dimensional materials.

The Seebeck coefficient in NWs depends at first order on the distance of the band edges form the Fermi level (η_F). At a constant carrier concentration η_F changes differently for different NW types as a function of diameter, mainly increasing with scaling (Fig. 3a). This increase improves the power factor as the diameter is reduced below D=7nm as shown in Fig. 3b (under ballistic conditions). Additionally, the carrier velocities are a strong function of NW type and can vary differently as the diameter is reduced. In some cases the carrier velocities are diameter independent (Fig. 3c), but in other cases they increase with diameter reduction (Fig. 3d).

Such property differences can be used to optimize the thermoelectric performance of NWs. For example, although under ballistic conditions the Seebeck coefficient can offer some advantages to the power factor, when phonon and surface roughness scattering (SRS) are considered, the conductivity is severely degraded with diameter reduction (Fig. 4a), and so is ZT (Fig. 4c). On the other hand, in cases where the carrier velocity increases with confinement, such as in p-type [111] NWs, the conductivity increases (Fig. 5a), which compensates for the effect of SRS and improved ZT values can be obtained (Fig. 5c).

CONCLUSION

Ultra-thin Si NWs offer the possibility of TE power factor optimization through bandstructure engineering techniques. The Seebeck coefficient and the electrical conductivity can be optimized using confinement and orientation to achieve enhanced TE properties.

ACKNOWLEDGEMENT

This work was supported by the Austrian Climate and Energy Fund, contract 825467.

REFERENCES

[1] A. I. Hochbaum et al., Nature, vol. 451, p. 163, 2008.
[2] A. I. Boukai et al., Nature, vol. 451, p.168, 2008.
[3] N. Neophytou and H. Kosina, PRB, 84, 085313, 2011.

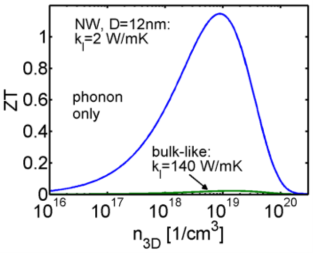

Fig. 1. The ZT figure of merit versus carrier concentration of a cylindrical NW of D=12nm calculated for k_l=2 W/mK (NW-like), and k_l=140 W/mK (bulk-like).

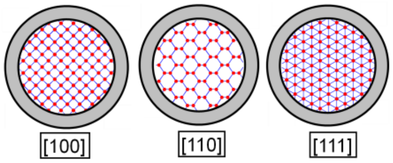

Fig. 2. Cross sections of the NWs analysed. The [100], [110] and [111] orientations. The NW surface is assumed to be hydrogen passivated.

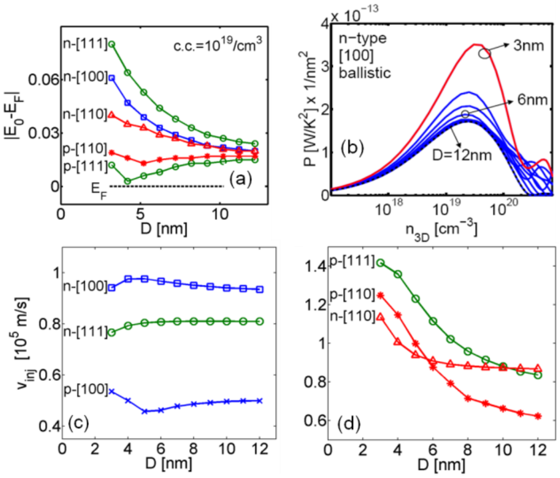

Fig. 3. (a) The shift in the band edge of n- and p-type NWs in different transport orientations vs. diameter, at carrier concentration 10^{19}/cm^3. (b) The power factor (ballistic) of n-type [100] NWs with D=12nm down to 3nm vs. carrier concentration. (c-d) The carrier injection velocities vs. diameter of n- and p-type NWs of different transport orientations.

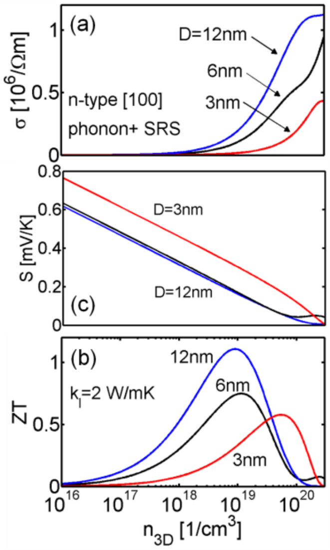

Fig. 4. Thermoelectric coefficients versus carrier concentration for n-type [100] NWs of D=12nm (blue), 6nm (black) and 3nm (red), at 300K. Phonon scattering plus SRS are included. (a) The electrical conductivity. (b) The Seebeck coefficient. (c) The ZT figure of merit (k_l=2 W/mK is assumed for all cases).

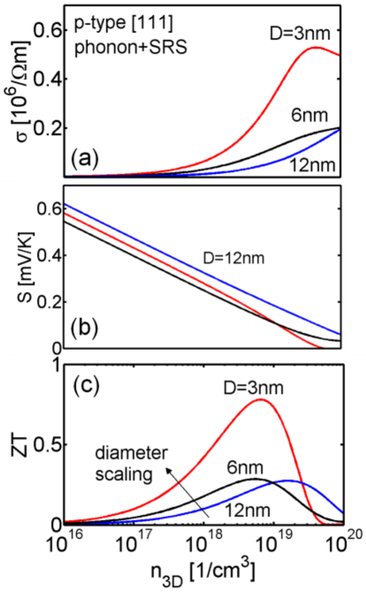

Fig. 5. Thermoelectric coefficients versus carrier concentration for p-type [111] NWs of D=12nm (blue), 6nm (black) and 3nm (red), at 300K. Phonon scattering plus SRS are included. (a) The electrical conductivity. (b) The Seebeck coefficient. (c) The ZT figure of merit (k_l=2 W/mK is assumed for all cases).